Band structure and omnidirectional photonic band gap in lamellar structures with left-handed materials

D. Bria,[1,2] B. Djafari-Rouhani,[2] A. Akjouj,[2,*] L. Dobrzynski,[2] J. P. Vigneron,[3] E. H. El Boudouti,[1,2] and A. Nougaoui[1]

[1]*Laboratoire de Dynamique et d'Optique des Matériaux, Département de Physique, Faculté des Sciences,*
Université Mohamed I, 60000 Oujda, Morocco
[2]*EDI, UMR CNRS 8024, UFR de Physique, Université de Lille I, 59655 Villeneuve d'Ascq, France*
[3]*Facultés Universitaires Notre Dame de la Paix, Rue de Bruxelles 61, B-5000 Namur, Belgium*

We theoretically investigate the photonic band structure of one-dimensional superlattices composed of alternating layers of right-handed and left-handed materials (RHM and LHM). The dispersion curves are mainly studied by assuming that the dielectric permittivity and magnetic permeability are constant in each layer. It is shown that such structures can exhibit new types of electromagnetic modes and dispersion curves that do not exist in usual superlattices composed only of RHM. In particular, we emphasize the possibility of bands that originate from the interface modes localized at the boundary between a LHM and RHM or from confined modes in one type of layers. These waves are evanescent in both or in one constituent of the superlattice. One of the pass bands may lie below the light lines of the constituting material and go down to the static limit of a vanishing frequency ω, even at a value of the wave vector $k_{\parallel}$ (parallel to the layers) that is different from zero. For a given value of the wave vector $k_{\parallel}$, the dispersion curves ω versus k_z (where k_z is the Bloch wave vector of the periodic system along the axis of the superlattice) may exist only in a limited part of the superlattice Brillouin zone and exhibit a zigzag behavior instead of a monotonic behavior as in usual superlattices. With an appropriate choice of the parameters, we show that it is possible to realize an absolute (or omnidirectional) band gap for either transverse electric (TE) or transverse magnetic (TM) polarization of the electromagnetic waves. A combination of two multilayer structures composed of RHM and LHM is proposed to realize, in a certain range of frequency, an omnidirectional reflector of light for both polarizations.

I. INTRODUCTION

Left handed materials (LHM's), in which the dielectric permittivity ε and magnetic permeability μ are simultaneously negative, have received a great deal of attention during the last few years [1]. This is due to the unusual physical properties of these materials that have raised strong theoretical interest and may lead to potential applications in optical devices. Some peculiar properties of LHM have already been discussed some thirty years ago by Veselago [2], for instance, a Poynting vector directed opposite to the propagation wave vector k, the reversal of Doppler and Cerenkov effects. Because of the absence of naturally existing LHM, the experimental realization of an artificial heterogeneous medium exhibiting both negative $\varepsilon(\omega)$ and $\mu(\omega)$ was performed only recently [3]. The realization of such media [3,4] are based on the propositions of Pendry *et al.* for specific structures [5]. Recent interest in these metamaterials has been directed towards the theoretical and experimental study of Snell's law of refraction at the boundary with a LHM [6–10], the focusing and imaging properties of a metamaterial lens [11–13], the tunneling in the presence of a LHM layer [14], the emission in a LHM metamaterial [15], etc.

Assuming the possibility of realizing such LHM under the form of layered media, a few recent works have investigated the photonic band structure of one dimensional layered structures constituted by a periodical repetition of RHM and LHM [16–18]. Some peculiar properties related to the presence of LHM layers have been underlined, for instance, the possibility of gap widening with respect to usual superlattices constituted only by RHM [16], the theoretical and experimental investigation of a new type of gap when the average index of refraction in the superlattice vanishes [17], and the possibilty of discrete and photon tunneling modes [18]. These works have mainly concentrated on propagation along the axis of the superlattice, i.e., normal incidence.

The object of this paper is to present theoretically a detailed study of the dispersion relation and photonic band structure in superlattices constituted by alternate layers of LHM and RHM, with the aim of giving the different trends that can occur and emphasizing the new behaviors that have not been predicted before. We present and discuss the band structure with various physical parameters and different ratios of the LHM to RHM layer thicknesses. In these calculations, the dielectric permittivity ε and magnetic permeability μ are, in general, assumed to take constant values. Although these parameters in LHM are in general frequency dependent, our results can be used to design specific metamaterials that would lead to a typical behavior around a given frequency. We also illustrate the photonic band structure in a case with frequency-dependent parameters. We discuss, in particular, the photonic bands of the superlattice originating from the interface modes at the boundary between a RHM and a LHM, and those bands that are confined in one type of layer in the superlattice. When the permittivity

*Electronic address: abdellatif.akjouj@univ-lille1.fr

ε and permeability μ are constant parameters, one of the pass bands can decrease down to the static limit of the frequency $\omega=0$ at a value of the wave vector $k_{\parallel}$, parallel to the layers, that is different from zero. For fixed values of $k_{\parallel}$, we also investigate the dispersion curves ω versus k_z, where k_z is the Bloch wave vector along the axis of the superlattice which is limited to the reduced Brillouin zone $-\pi/D < k_z < \pi/D$ (D being the period of the superlattice). In contrast to the case of usual superlattices where ω displays a monotonic variation with k_z, while k_z goes from 0 to π/D and vice versa, in the LHM-RHM composite superlattices some of the dispersion curves may exist only in a limited part of the Brillouin zone and even display a zigzag behavior.

We also show that for some particular choices of the physical and geometrical parameters, the RHM-LHM superlattice can exhibit an absolute (or omnidirectional) band gap, for either TE or TM polarization of the electromagnetic field. This situation is without analog in the case of usual superlattices. Thus, a combination in tandem of two LHM-RHM superlattices enable us to propose an omnidirectional reflector structure for both polarizations of the light. Let us notice that the search of omnidirectional reflection gaps has been the object of several recent works [16,19–23]. In particular, the possibility of an omnidirectional reflection gap in a lamellar structure containing left handed media has been mentioned in Ref. [16]

The paper is organized as follows. For the clarity of the discussion, we briefly present in Sec. II the interface modes localized at a LHM-RHM boundary as well as the confined modes of a LHM layer embedded between two semi-infinite RHM media. Section III is devoted to the presentation of our main results as concerns the photonic band structure of LHM-RHM superlattices. Finally, some conclusions are drawn in Sec. IV.

Let us notice that the derivation of the single interface mode and the modes in a slab of LHM have been considered in two recent papers by Ruppin [24,25]. Therefore, the object of Sec. II is mainly to emphasize the physical behaviors in these two problems for a clear understanding of the results presented in Sec. III.

II. INTERFACE MODES AND CONFINED MODES OF A LAYER

In the following, we assume that the z axis is along the normal to the interfaces and the wave vector component parallel to the layers $k_{\parallel}$ is along the x axis. From the Maxwell's equations in each medium, it is straightforward to write the electromagnetic field of TE polarization under the form

$$E_y = (Ae^{\alpha z} + Be^{-\alpha z})e^{i(k_{\parallel}x - \omega t)},$$

$$B_x = \frac{i\alpha}{\omega}(Ae^{\alpha z} - Be^{-\alpha z})e^{i(k_{\parallel}x - \omega t)}, \qquad (1)$$

$$B_z = \frac{k_{\parallel}}{\omega}(Ae^{\alpha z} + Be^{-\alpha z})e^{i(k_{\parallel}x - \omega t)},$$

where $\alpha = \sqrt{k_{\parallel}^2 - \varepsilon\mu(\omega^2/c^2)}$, c is the speed of light in vacuum, ε and μ are the relative dielectric permittivity and magnetic

permeability of the material, and the index of refraction is defined by $n = \pm\sqrt{\varepsilon\mu}$ with the plus or minus sign being used, respectively, for RHM and LHM. Similar equations can be written for electromagnetic waves of TM polarization for which the nonzero components of the field are B_y, E_x, E_z. In lamellar structures, it is also necessary to satisfy the boundary conditions at each interface, namely, the continuity of the tangential components of $\vec{E}$ and $\vec{H}$ and of the normal components of $\vec{D}$ and $\vec{B}$.

First, we are interested by the interface modes localized at the boundary $z=0$ between a LHM and a RHM (see also Ref. [24]). Such a wave should be exponentially decaying on both sides of the interface and, therefore, its frequency lies below the light lines of both media (i.e., both α_1 and α_2 are real, where the indices 1 and 2 refer to the media on both sides of the interface). Keeping in the above field [Eq. (1)] in each of the media 1 and 2, only the exponential term which is decaying far from the interface and using the boundary conditions at $z=0$, one easily obtains the equation giving the interface modes, namely,

$$F_1 + F_2 = 0, \qquad (2)$$

where $F_i = (\alpha_i/\mu_i)(i=1,2)$ for TE modes, and $F_i = -(\varepsilon_i/\alpha_i) \times (\omega^2/c^2)$ for TM modes [26]. The parameters F_i are proportional to the electromagnetic admittance of the corresponding materials for each polarization. By taking the squares in these equations, it is possible to solve for the frequency ω and obtain

$$\frac{c^2 k_{\parallel}^2}{\omega^2} = \frac{\dfrac{\varepsilon_1}{\mu_1} - \dfrac{\varepsilon_2}{\mu_2}}{\dfrac{1}{\mu_1^2} - \dfrac{1}{\mu_2^2}}$$

for TE modes and

$$\frac{c^2 k_{\parallel}^2}{\omega^2} = \frac{\dfrac{\mu_1}{\varepsilon_1} - \dfrac{\mu_2}{\varepsilon_2}}{\dfrac{1}{\varepsilon_1^2} - \dfrac{1}{\varepsilon_2^2}}$$

for TM modes. However, it should be pointed out that these solutions are valid provided the slope $\omega/k_{\parallel}$ of the corresponding lines remain below the velocities of light in both media 1 and 2. Thus, one can easily derive the condition for the existence of interface modes as follows: For TE modes: either $\varepsilon_2\mu_2 < \varepsilon_1\mu_1$ and $\mu_2^2 > \mu_1^2$ or $\varepsilon_2\mu_2 > \varepsilon_1\mu_1$ and $\mu_2^2 < \mu_1^2$; for TM modes: either $\varepsilon_2\mu_2 < \varepsilon_1\mu_1$ and $\varepsilon_2^2 > \varepsilon_1^2$ or $\varepsilon_2\mu_2 > \varepsilon_1\mu_1$ and $\varepsilon_2^2 < \varepsilon_1^2$.

Unlike the case of an interface between two RHM, the RHM-LHM interface can support a localized mode of TE polarization. However, one can notice that the TE and TM interface localized modes can never exist simultaneously, i.e., the interface supports at most one localized mode of either TE or TM polarization.

Now, we are interested by the confined modes of a LHM layer of medium 2, extending in the region $0 < z < d$, embedded between two semi-infinite RHM made of material 1 (see
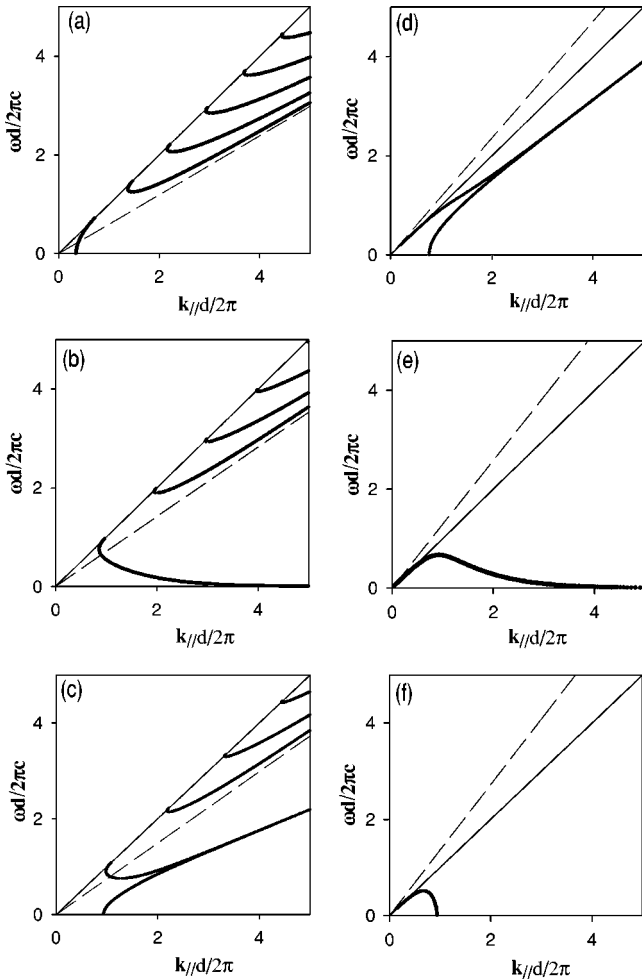
FIG. 1. Dispersion curves of confined TE optical modes in LHM layer of thickness d sandwiched between vacuum. The parameters $[\varepsilon; \mu]$ of LHM are taken to be (a) $[-1.4; -2]$, (b) $[-2; -1]$, (c) $-2; -0.9$, (d) $-0.6; -1.2$, (e) $-0.6; -1$, and (f) $-0.6; -0.9$. The reduced frequency $\Omega = \omega d / 2\pi c$ is presented as a function of the reduced wave vector $\kappa_{\parallel} = k_{\parallel} d / 2\pi$. The straight lines show the light lines of vacuum (full line) and of the LHM layer (dashed line).

also Ref. [25]). The confined modes of the layer are obtained by writing the solution of Maxwell's equations as propagating waves inside the layer and decaying waves outside the layer and using the usual boundary conditions at both interfaces $z=0$ and $z=d$. The dispersion relations derive straightforwardly as

$$(F_1^2 + F_2^2)\sinh(\alpha_2 d) + 2F_1 F_2 \cosh(\alpha_2 d) = 0. \tag{3}$$

In Fig. 1, we show all possible behaviors of the TE modes dispersion curves by choosing different parameters for the LHM layer, the RHM medium being vacuum. Let us emphasize that we obtain similar results for TM modes since the results for one polarization can be transposed to the other by interchanging the parameters ε_i and μ_i. Also, exactly the same behaviors are observed if a finite RHM layer is embedded between two semi-infinite LHM's, so for the sake of briefness we escape these results. In Fig. 1, we have presented the confined modes of the embedded LHM layer, so

all the dispersion curves lie below the light line of the external medium, i.e., vacuum in our case. The panels (a), (b), (c) in the left column [(d), (e), (f) in the right column] refer to a LHM material with an index of refraction $|n_2|$ greater (smaller) than $n_1 = 1$. The panels in the upper, middle, and lower rows, respectively, correspond to a LHM material with $|\mu_2|$ greater than, equal to, or smaller than $\mu_1 = 1$.

In the example of panel (a) where $|\mu_2| > 1$, most of the confined modes resemble those of the usual RHM. In particular, for increasing wave vector $k_{\parallel}$, the slopes of the dispersion curves go to the velocity of light in medium 2. Still, one can observe a nonmonotonic behavior of the dispersion curves around their crossing points with vacuum light line. However, the main novelty in this figure is the existence of the lower branch that starts at $\omega = 0$ for a wave vector $k_{\parallel}$ different from zero. In the limit of $\omega = 0$, the solution for the electromagnetic field reduces to a static magnetic field while the electric field should be equal to zero to prevent the divergence of the magnetic field [see Eq. (1)]. In panel (c), the parameters are chosen in such a way that the RHM-LHM interface can support a localized mode ($|\mu_2| < 1$). Thus, in addition to the confined modes of the layer, one can observe two degenerate interface modes in the limit of large $k_{\parallel} d$ (see the two lowest dispersion curves); this degeneracy is lifted at lower values of $k_{\parallel} d$ where the corresponding modes can interact together due to the proximity of the interfaces. Thus, for small values of $k_{\parallel} d$, these modes become more spread over the entire layer and less localized around the interfaces $z = 0$ and $z = d$. Panel (b) corresponds to an intermediate case between the examples of panels (a) and (c), namely, $\mu_2 = -1$. In this case, the interface mode ceases to exist, but there is a dispersion curve which goes asymptotically to $\omega = 0$.

The examples sketched in panels (d), (e), and (f) (right column of Fig. 1) correspond to an index of refraction $|n_2|$ in the LHM lower than 1, so the light line of medium 2 is above the vacuum light line. Consequently, the dispersion curves of the confined modes can be searched for only below the latter line. In case (d) where $|\mu_2| > 1$, the dispersion curves display two branches that become the localized interface modes at the LHM-RHM boundaries in the limit of large $k_{\parallel} d$; for decreasing $k_{\parallel} d$, the two interface modes interact more strongly and their degeneracy is lifted. In case (f) where $|\mu_2| < 1$, the RHM-LHM interface does not support any localized mode, so a dispersion curve appears only in a limited range of the wave vector $k_{\parallel}$. Finally, case (e) where $\mu_2 = -1$ is intermediate between cases (d) and (f), i.e., there is one dispersion curve going asymptotically to $\omega = 0$.

In the next section, we shall study the photonic band structure of a periodic stack of LHM-RHM layers. The bands that will appear below the light lines of either media 1 or 2 are those resulting from the interaction of the confined modes discussed above. Therefore, some new behaviors are expected with respect to usual RHM-RHM superlattices in relation with the dispersion curves sketched in Fig. 1.

III. PHOTONIC BAND STRUCTURE OF A LHM-RHM SUPERLATTICE

We shall call d_1 and d_2 the thicknesses of layers 1 and 2, respectively, with $D = d_1 + d_2$ being the period of the superlat-

tice. In the examples presented in this section, medium 1 is vacuum whereas medium 2 is a LHM with different dielectric permittivity and magnetic permeability. The derivation of the dispersion relation of the superlattice is quite simple and well known. First, one can write the solutions of the Maxwell equations in each medium under the form of Eq. (1). Then, we use the periodicity of the system to introduce a Bloch wave vector k_z along the axis of the superlattice that relates the field in two consecutive unit cells by the factor e^{ik_zD} (remember that k_z is limited to the first Brillouin zone $-\pi/D < k_z < \pi/D$). In this way, there are four unknown coefficients A_1, B_1 and A_2, B_2 (two in each type of layer). Finally, one has to write the four boundary conditions at two consecutive interfaces that give rise to a system of four linear homogeneous equations for the unknown coefficients. By setting the determinant of this system equal to zero, one obtains the following dispersion relation:

$$\cos(k_zD) = \cosh(\alpha_1d_1)\cosh(\alpha_2d_2)$$
$$+ \frac{1}{2}\left(\frac{F_1}{F_2} + \frac{F_2}{F_1}\right)\sinh(\alpha_1d_1)\sinh(\alpha_2d_2). \quad (4)$$

The expressions of F_i for both TE and TM polarizations were given in Sec. II. The dispersion relation (4) can be solved in the following way. The right-hand side of Eq. (4) is evaluated for any values of ω and $k_\parallel$. If the result is smaller than 1 in absolute value, one can obtain a real solution for k_z, i.e., the corresponding wave propagates along the axis of the superlattice and ω belongs to a pass band for the chosen value of $k_\parallel$. Otherwise, k_z becomes a complex number, the wave cannot propagate and ω belongs to a gap of the superlattice. The dispersion curves can be sketched in two different ways. One way is to fix the wave vector component $k_\parallel$ and give the frequency ω as a function of the Bloch wave vector k_z. In the other way, the so-called projected band structure is presented in which all the pass bands and minigaps are displayed as a function of $k_\parallel$. In Figs. 2 and 3, we give these two types of illustrations in a few cases that cover most of the possible behaviors for the RHM-LHM superlattice photonic band structure. In these figures, the parameters of material 2 are taken to be $\varepsilon_2=-0.6$ and $\mu_2=-1$, whereas a few values are given to the volume fraction d_2/D of this medium. The results are presented as a function of dimensionless frequency $\Omega=\omega D/2\pi c$ and dimensionless wave vectors $\kappa_\parallel=k_\parallel D/2\pi$ and $\kappa_z=k_z D/2\pi$. The results presented in Figs. 2 and 3 are complementary; nevertheless, we have given the band structures of Fig. 3 for both TE (right side of Fig. 3) and TM (left side of Fig. 3) polarizations whereas, for the sake of briefness, the dispersion curves of Fig. 2 are presented only for TM modes.

Figure 2 shows the dispersion curves Ω versus κ_z for three different values of $\kappa_\parallel$ [namely, $\kappa_\parallel=0.5$ (left column), $\kappa_\parallel=0.7$ (middle column), and $\kappa_\parallel=2.5$ (right column)] and for three values of the filling fraction d_1/D [namely, $d_1/D=0.3$ (upper row), 0.43649 (middle row), and 0.5 (lower row)]. The value 0.43649 of the filling fraction is the one for which the average index of refraction in the superlattice $\langle n \rangle = (d_1n_1+d_2n_2)/D$ becomes equal to zero; it leads to peculiar behaviors of the dispersion curves (see below) that have also

been discussed in Refs. [16–18], mainly at $\kappa_\parallel=0$.

In panel (a) of Fig. 2, the dispersion curves behave similarly to the usual case of superlattices made only of RHM. By changing slightly $\kappa_\parallel$, a new dispersion curve starts to emerge around $\Omega=0$ and $\kappa_z=0$ [see the lowest branch in panel (b)], that extends only over a limited range of the reduced Brillouin zone. Increasing further $\kappa_\parallel$, the latter branch covers the whole range of the Brillouin zone and even (see panel (c)] a cutoff frequency appears. Let us notice that this branch is situated below the light lines of the media constituting the superlattice in panel (b) but moves above these lines in panel (c). A global view of these results can be seen in the projected band structure displayed in Fig. 3(a) (left side) where the shaded area correspond to the pass bands and the white area to the gaps. The novel behavior resulting from the presence of the LHM is the existence of a pass band that falls below the light lines of both media in the superlattice and reaches the frequency $\omega=0$ for nonvanishing values of the wave vector $k_\parallel$. This band results from the interaction between the confined modes [see the lowest branch in Fig. 1(e)] in different layers of the superlattice. This behavior is without analog in the case of usual superlattices made of RHM.

Another type of behavior for the dispersion curves is presented in the second row of Fig. 2 [see also Fig. 3(c)], corresponding to a filling fraction $d_1/D=0.43649$ such that the average index of refraction in the superlattice vanishes, $d_1n_1+d_2n_2=0$. It has been argued [17] that for this choice of the filling fraction, the propagation along the axis of the superlattice, i.e., for $\kappa_\parallel=0$, becomes prohibited except at some discrete values of the frequency (see also Refs. [16,18]). This can be clearly seen in the projected band structure of Fig. 3(c), where the consecutive gaps join together to constitute a very large gap. Now, when $\kappa_\parallel$ departs from zero, the gaps become separated by very narrow bands, i.e., the discrete modes transform into narrow bands [see panels (d) and (e) in Fig. 2] in which the wave vector κ_z describes a small region around $\kappa_z=0$, whereas the lowest dispersion curve extends over a more or less spread domain of the Brillouin zone. For higher values of $\kappa_\parallel$ [see panel (f) of Fig. 2 and also Fig. 3(c)], the pass bands widen and some of them join together to constitute a continuous band. Therefore the occurrence of narrow bands and discrete modes is related to the fact that some of the band gaps join together and the pass bands that separate them close.

A third example of the dispersion curves is presented for the filling fraction $d_1/D=0.5$ [third row of Figs. 2 and 3(d)]. At $\kappa_\parallel=0$, these curves are again similar to those of usual superlattices. However, by increasing $\kappa_\parallel$ [see panels (g) and (h) of Fig. 2], the lowest curve covers only a limited part of the Brillouin zone; more especially, for increasing Ω, this curve starts from $\kappa_z=0.5$ and returns back to the same wave vector, displaying a zigzag behavior. The width of the corresponding pass band, that extends over the frequency range $0.4 < \Omega < 4.2$ at $\kappa_\parallel=0.7$ [panel (h)], can be reduced very much when $\kappa_\parallel$ increases up to 1.8 where the band approaches the limit of a discrete mode. Panel (i), corresponding to $\kappa_\parallel=2.5$ also shows a zigzag type of behavior, but now for a dispersion curve starting from, and ending at, $\kappa_z=0$. A global view of these results are presented in the projected band
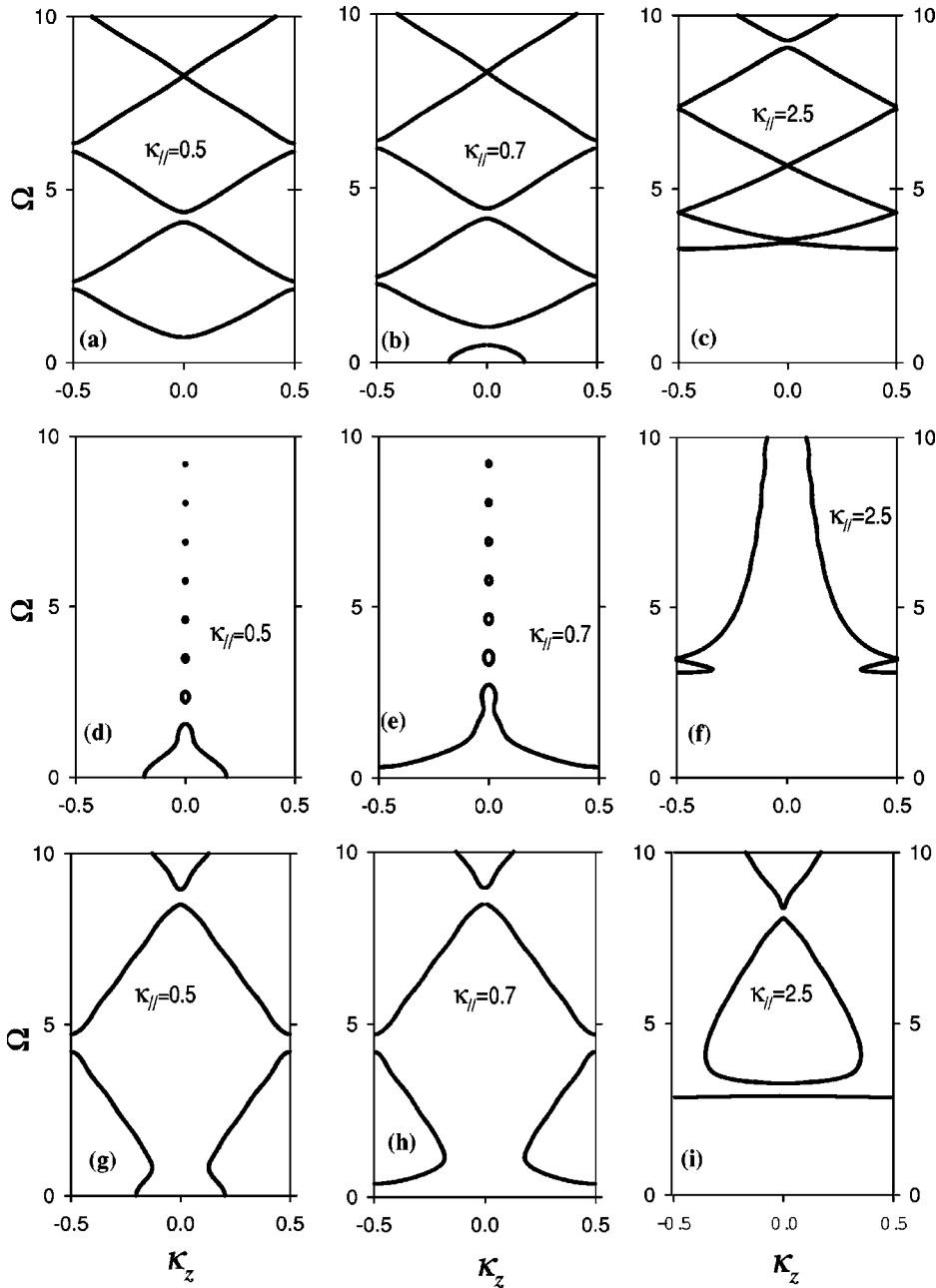
FIG. 2. Dispersion curves of a vacuum-LHM superlattice for different values of the wave vector component $k_\parallel$, parallel to the layers, and different volume fraction of vacuum d_1/D. The parameters of LHM are $\epsilon_2 = -0.6$, $\mu_2 = -1$. The reduced frequency $\Omega = \omega d/2\pi c$ is presented as function of the reduced wave vector $\kappa_z = k_z D/2\pi$. The panels in the upper, middle and lower rows, respectively, correspond to $d_1/D = 0.3$, 0.43649 and 0.5. The panels in the left, middle, and right columns refer, respectively, to the dimensionless wave vector parallel to the layers $\kappa_\parallel = k_\parallel d/2\pi = 0.5$, 0.7, and 2.5.

structure of Fig. 3(d) (left side). Here again, one can recognize a pass-band situated below the light lines of the constituting materials in the superlattice. The occurrence of very narrow bands and discrete modes mentioned above can be more clearly seen in the TE band structure of Fig. 3(d) (right side). For instance, one can notice that at $\kappa_\parallel \approx 1.84$ two band gaps, delimited by loop shaped curves, join together around the frequency $\Omega \approx 3.52$. Therefore around these values of $\kappa_\parallel$ and Ω, there is a very narrow band that separates the two gaps; this pass band goes to the limit of a discrete mode at the particular value of $\kappa_\parallel$ where the gaps join together and the width of the pass band vanishes. However, looking to the dispersion curves Ω versus κ_z, the narrow band extends only over a very limited range of the Brillouin zone, namely, κ_z starts and ends at $\kappa_z = 0.5$ while remaining always in the near vicinity of the Brillouin zone edge.

Now, let us make a few complementary comments about the projected photonic band structures which is displayed in Fig. 3 for several values of the filling fraction, namely, $d_1/D = 0.3$ (a), 0.4 (b), 0.43649 (c), 0.5 (d), 0.65 (e), and 0.8 (f). First, one can notice a number of narrow bands situated between the light lines of vacuum and the LHM. These bands result from the interaction of confined modes of vacuum layer embedded between two LHM's (we remember that in our example the vacuum light line is below the LHM light line). Thus, the number of these bands increases with the filling fraction d_1/D of vacuum layers [from panel (a) to panel (f)]. The other point to notice is about the different trends that can be observed around the frequency zero. Referring to TM polarization (left side of the figure), in panel (a) there is a band reaching $\Omega = 0$ over a range of the wave vector $\kappa_\parallel$ outside zero. A triangular gap separates this band
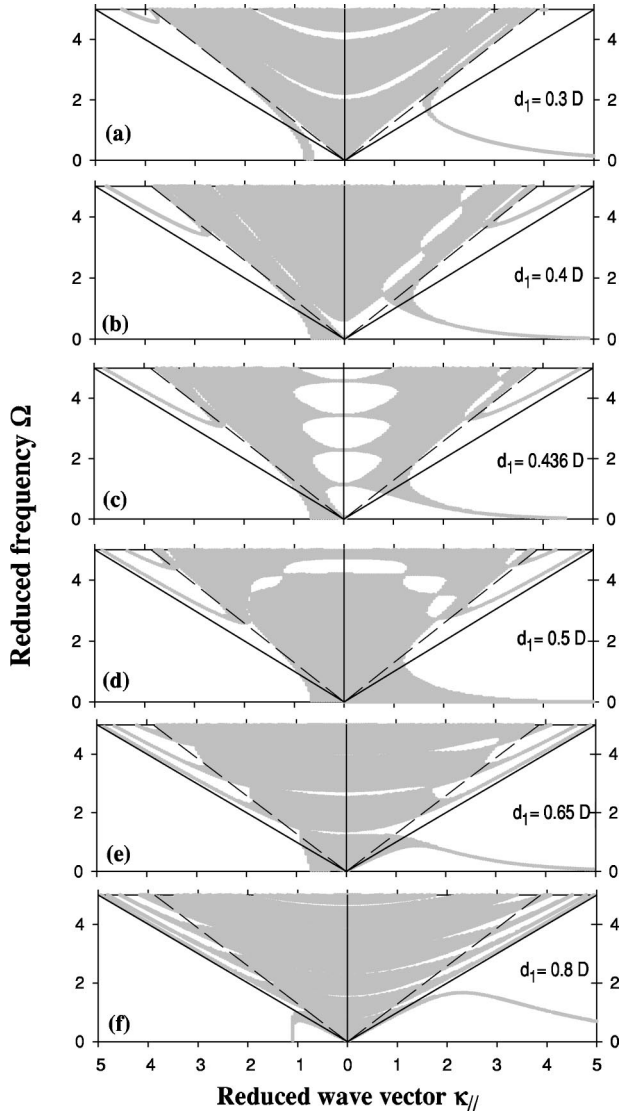
FIG. 3. Projected photonic band structure of a vacuum-LHM superlattice for different values of the volume fraction of vacuum d_1/D. The reduced frequency $\Omega = \omega d/2\pi c$ is presented as a function of the reduced wave vector $\kappa_\| = k_\| d/2\pi$. The shaded and white areas respectively correspond to the pass bands and to the gaps of the superlattice. The left and right sides of the figures, respectively, give the band structures of the TM and TE modes. The parameters of LHM are $\epsilon_2 = -0.6$, $\mu_2 = -1$. The filling fraction d_1/D takes the following values in the different panels: (a) 0.3, (b) 0.4, (c) 0.43649 (corresponding to $\langle n \rangle = 0$), (d) 0.5, (e) 0.65, and (f) 0.8. The straight lines show the light lines of vacuum (full line) and of LHM (dashed line).

from the next band that starts at $\kappa_\| = 0$. Increasing the filling fraction [panel (b)], the former band reaches $\kappa_\| = 0$ while the latter have moved to a nonvanishing value of the frequency Ω. Increasing further the filling fraction, both bands merge together [panels (d) and (e)]. For even higher filling fraction, we find the situation of panel (f) where the lowest band bends downwards to reach $\Omega = 0$ over a range of the wave vector $\kappa_\|$ outside zero.

The above discussion can be illustrated both analytically or numerically by looking to the trends of the dispersion
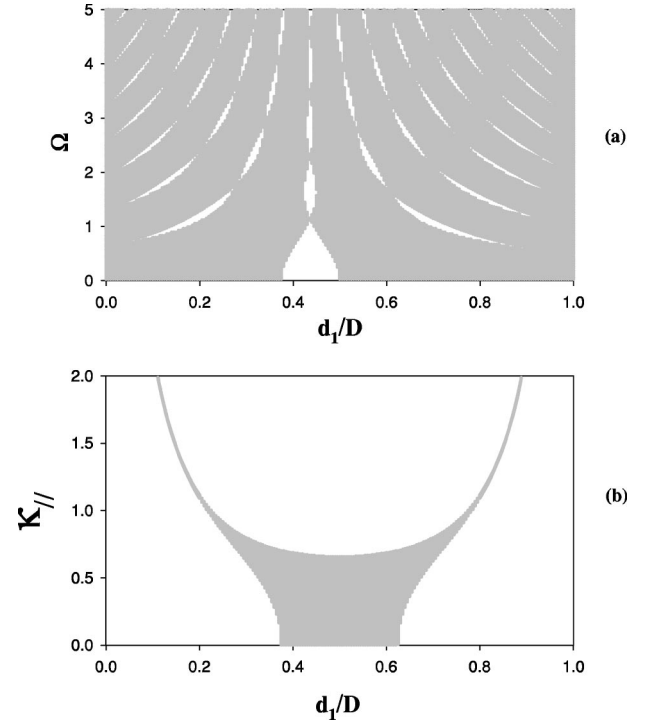
FIG. 4. (a) Frequencies of photonic bands at $\kappa_\| \equiv 0$ as a function of the filling fraction d_1/D in a vacuum-LHM superlattice. The parameters of LHM are $\epsilon_2 = -0.6$, $\mu_2 = -1$. The shaded and white areas, respectively, correspond to the pass bands and to the gaps of the superlattice. (b) Values of $\kappa_\|$ for which a photonic band exists at $\Omega = 0$ versus d_1/D.

relation (4) either along the axis Ω or along the axis $\kappa_\|$. To have an analytical insight about these behaviors, let us first assume that both $\kappa_\|$ and Ω are much smaller than 1. Then, we can make a Taylor expansion of Eq. (4) that yields

$$\cos(k_z D) \cong 1 - 4\pi^2 \langle \mu \rangle \langle \varepsilon \rangle \Omega^2$$
$$+ 4\pi^2 \left\langle \frac{1}{\varepsilon} \right\rangle \langle \varepsilon \rangle \kappa_\|^2 \text{ for TM modes} \quad (5a)$$

and

$$\cos(k_z D) \cong 1 - 4\pi^2 \langle \mu \rangle \langle \varepsilon \rangle \Omega^2$$
$$+ 4\pi^2 \left\langle \frac{1}{\mu} \right\rangle \langle \mu \rangle \kappa_\|^2 \text{ for TE modes.} \quad (5b)$$

In these equations the symbol $\langle A \rangle$ means the average of the quantity A, i.e. $\langle A \rangle = (d_1 A_1 + d_2 A_2)/D$. From the above Taylor expansions, it is easy to analyze the existence of gaps or pass bands around Ω and $\kappa_\| \sim 0$. Referring to TM polarization, for instance, and choosing $\Omega \equiv 0$, one can see from the right-hand side of Eq. (5a) that a pass band (a gap) exists along the $\kappa_\|$ axis if $\langle \varepsilon \rangle \left\langle \frac{1}{\varepsilon} \right\rangle$ is negative (positive). Similarly, by choosing $\kappa_\| \equiv 0$, one finds that a pass band (gap) occurs along the Ω axis if $\langle \varepsilon \rangle \langle \mu \rangle$ is positive (negative). We also illustrate these behaviors numerically in Fig. 4 by choosing either $\kappa_\| \equiv 0$ or $\Omega \equiv 0$. In Fig. 4(a), we present the photonic bands of the superlattice at $\kappa_\| \equiv 0$ as a function of the filling
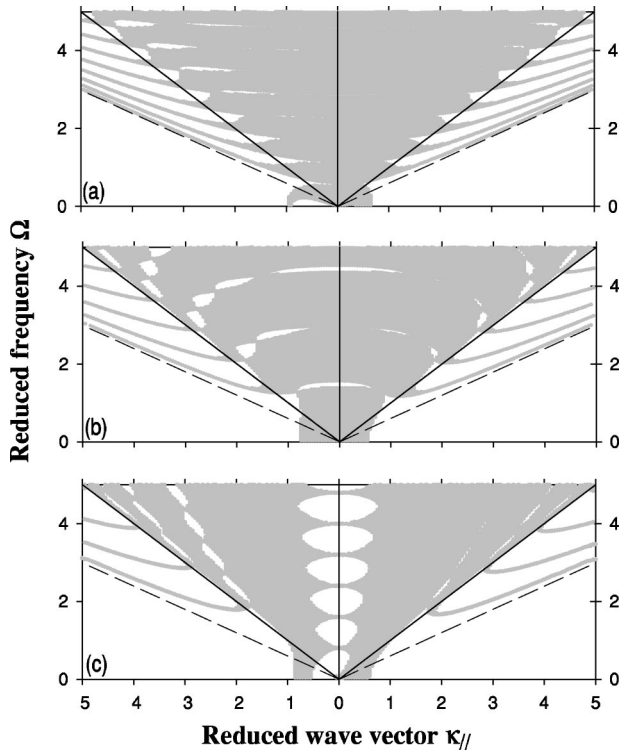
FIG. 5. Same as in Fig. 3 for the following parameters of LHM: $\epsilon_2 = -1.4$, $\mu_2 = -2$. In the different panels, the layer thicknesses are defined as $d_1 = 0.3D$(a), $d_1 = 0.5D$(b), and $d_1 = 0.62593D$ (corresponding to $\langle n \rangle = 0$).

FIG. 6. (a) Magnification of the projected band structure of Fig. 5(b) at the frequency of the TM absolute band gap ($\Omega \approx 0.55$). (b) Magnification of the projected band structure of Fig. 3(e) in the vicinity of the TE absolute band gap. All the thicknesses are scaled by a factor of 2.3 with respect to those of Fig. 3(e) in order to bring the TE and TM absolute gaps in coincidence. (c) Overlap of the band gaps displayed in panels (a) and (b) to show the frequency range in which the propagation will be prohibited through a structure resulting from a combination in tandem of two multilayers.

fraction d_1/D. Notice that at $\kappa_\parallel \equiv 0$ there is no distinction between TE and TM modes. In this figure, one can see that a frequency cutoff exists for a range of the filling fraction extending from 0.375 (where $\langle \epsilon \rangle = 0$) to 0.5 (where $\langle \mu \rangle = 0$). More particularly, at the filling fraction 0.43649, where $\langle n \rangle$ vanishes, the propagation becomes prohibited except at some discrete frequencies. In Fig. 4(b), we choose $\Omega \equiv 0$ and represent the TM photonic bands as a function of $\kappa_\parallel$. One can see that the pass band which reaches $\Omega = 0$ extends over a limited range of $\kappa_\parallel$ that either includes $\kappa_\parallel = 0$ (for $0.375 < d_1/D < 0.625$) or excludes it.

Although the above discussions of Figs. 2–4 were mainly concentrated on modes of TM polarization, it should be emphasized that the TE photonic band structure display qualitatively similar results to those of TM modes. The fact that in Fig. 3 the lowest TE band asymptotically goes to zero, instead of cutting the $\kappa_\parallel$ axis, is due to the choice of $\mu_2 = -1$ in our example. This is related to the behavior of the confined modes of a layer [see Fig. 1(e)] when $\mu_2 = -\mu_1$.

An interesting and unexpected result which is due to the presence of LHM layers is the existence in Fig. 3(e) of an absolute (or omnidirectional) band gap of TE polarization in the frequency range $1.22 < \Omega < 1.4$. Indeed, this frequency interval is free of TE modes for any value of the wave vector $\kappa_\parallel$. Consequently, a wave launched from any substrate with an arbitrary angle of incidence is prohibited from propagation and will be reflected back. The superlattice becomes a perfect mirror for the TE modes, or a filter for TM modes, in this frequency range. This situation is without analogue in

usual RHM superlattices where the photonic band structure never contains an absolute band gap and the property of omnidirectional reflection requires that the incident light is launched from a substrate in which the index of refraction is relatively lower than those of the materials composing the superlattice [22].

Let us mention that the authors of Ref. [16] have also reported the possibility of an omnidirectional reflection gap in a lamellar structure containing left handed media. The case studied in this paper should be similar to the one reported in our Fig. 3(c): in this figure, a given frequency situated in the lowest gap is omnidirectional reflective for TE polarization, provided the incident light is launched from a substrate in which the index of refraction does not exceed a certain limit. However, in contrast to the case of Fig. 3(e) [see also Fig. 6(b)], Fig. 3(c) does not display any absolute gap, this means that the band structure does not contain any frequency range which remains free of a mode for any value of the wave vector $\kappa_\parallel$.

Another illustration of the projected photonic band structures is given in Fig. 5 for a superlattice in which the parameters of LHM are $\varepsilon_2 = -1.4$ and $\mu_2 = -2$ and the RHM is still vacuum. Although the velocity of light in the LHM is here lower than c, the results are overall qualitatively similar to those of Fig. 3. The narrow bands between the light lines of the constituting materials are now originating from the confined modes of the LHM layers embedded between vacuum. One can also notice the existence of a band that reaches $\Omega = 0$ for $\kappa_\parallel$ different from zero, as well as the peculiar behavior of the band structure at a filling fraction such that $\langle n \rangle = 0$
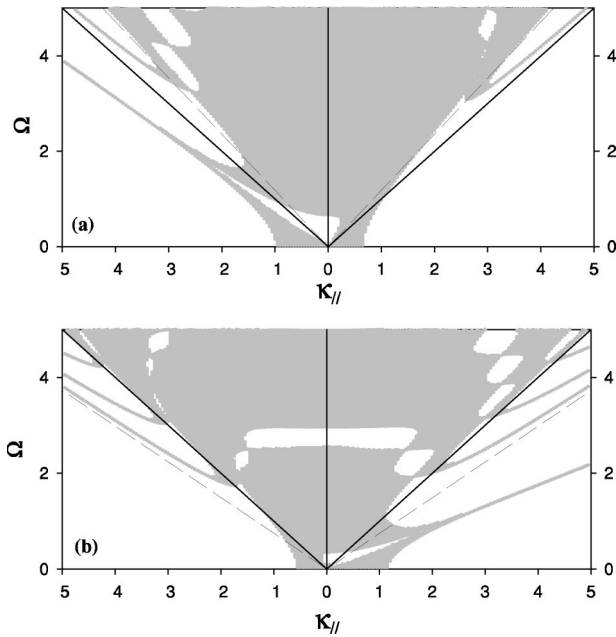
FIG. 7. Same as in Fig. 3, for the following parameters of LHM: (a) $[\varepsilon_2=-1.2;\mu_2=-0.6]$ and (b) $[\varepsilon_2=-2;\mu_2=-0.9]$ (b). In both cases, the thickness d_2 of the LHM layers is equal to $0.5D$.

[panel (c)]. An interesting result of Fig. 5(a) is the existence of an absolute band gap of TM polarization that extends in the frequency interval $0.54<\Omega<0.61$ while such an omnidirectional gap cannot exist in usual RHM superlattices.

In the previous examples of Figs. 3 and 5, we have shown that for an appropriate choice of the material parameters and their volume fraction, the LHM-RHM can display an omnidirectional gap for either TE or TM polarization. Now, by making a combination in tandem of two such multilayer structures [22,23], it should be possible to realize in a certain frequency range an omnidirectional reflector of light for both polarizations. This operation is sketched in Fig. 6. The upper panel is just a magnification of the TM absolute gap of Fig. 5(a). The middle panel is a magnification of the TE absolute gap of Fig. 3(e); however, the layer thicknesses d_1 and d_2 and the period D of the superlattice are multiplied here by a factor of 2.3 in order to obtain the coincidence of the TE and TM gaps. The lower panel in Fig. 6 shows the frequency domain in which the propagation is prohibited for both polarizations when the band gaps of panels (a) and (b) are superimposed. Of course, in a real structure the number of periods in each superlattice is finite and a small part of an incident signal will be transmitted. It would be necessary to investigate the decaying of the transmitted wave as a function of the total thicknesses of the multilayer structures, as we did in our previous works dealing with RHM materials [22] or with acoustic waves [23].

A third example of the projected photonic band structure is given in Fig. 7 with the following parameters of the RHM: (a) $\varepsilon_2=-1.2$, $\mu_2=-0.6$ and (b) $\varepsilon_2=-2$, $\mu_2=-0.9$. The filling fraction is taken to be 0.5. The novelty in this case with respect to the previous illustrations is the existence of a narrow band that originates from the interface mode at the RHM-LHM boundary. This band, which is either of TM
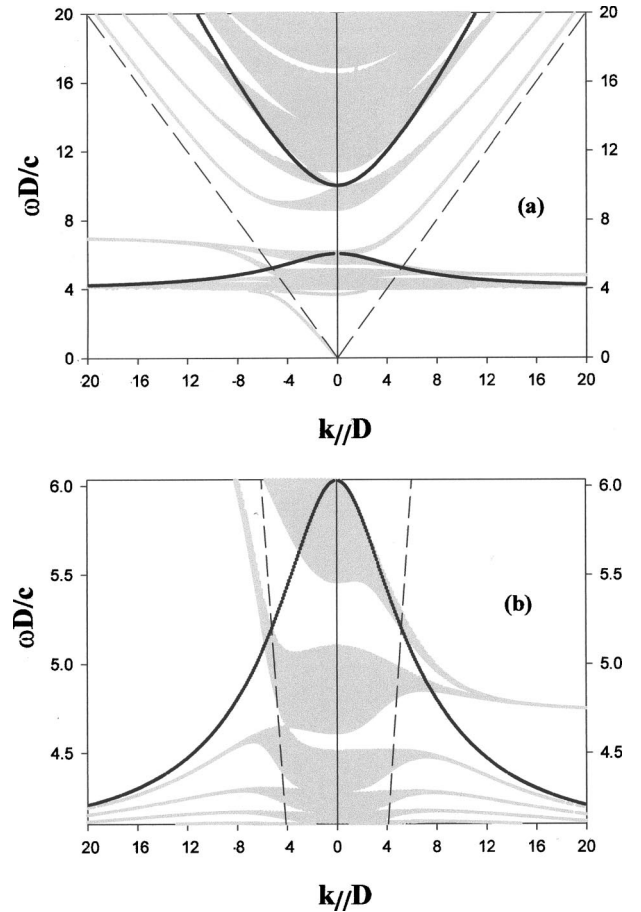
FIG. 8. (a) Same as in Fig. 2 when ε_2 and μ_2 are defined by Eq. (6). (b) Magnification of Fig. 8(a) in the frequency range $\omega D/c \sim 4$ to 6 where both ε_2 and μ_2 are negative. The straight dashed line is the vacuum light line. The heavy solid lines, defined by the equation $\alpha_2=0$, separate the regions of propagative and evanescent waves in LHM.

[panel (a)] or TE [panel (b)] polarization, is situated below the light lines of both materials and becomes similar to a straight line in the limit of high $\kappa_{\parallel}$. For small $\kappa_{\parallel}$, it widens and can divide into two different bands. From the discussion of Sec. II, let us remember that it is not possible to obtain the interface band simultaneously for TE and TM polarizations.

Finally, in Fig. 8 we illustrate the photonic band structure for a superlattice in which the parameters ε_2 and μ_2 of the LHM are frequency dependent and take the following forms [17,24,25]:

$$\varepsilon_2(\omega) = 1 - \frac{\omega_p^2}{\omega^2}, \quad \mu_2(\omega) = 1 - \frac{F\omega^2}{\omega^2-\omega_0^2}. \quad (6)$$

In this figure, we have chosen $\omega_p D/c=10$, $\omega_0 D/c=4$, $F=0.56$, and $d_1=d_2=D/2$. The heavy solid lines are obtained by putting $\alpha_2=0$ in LHM, i.e., these curves separate the regions of propagating and evanescent waves in LHM. The evanescent waves appear in the region between the two curves. The dashed straight line is the vacuum light line. The band structure is magnified in the frequency range $4 \leqslant \omega D/c \leqslant 6$ [Fig. 8(b)] where both ε_2 and μ_2 are negative.

The following points should be emphasized. For $k_{\parallel}D$ going to infinity, there are two bands of TE polarization around $\omega D/c \simeq 4.75$ [see Fig. 8(b)] which are separated from each other by a very small gap (not visible at the scale of the figure). These bands originate from the interface mode at the LHM-vacuum boundary; they broaden when $k_{\parallel}D$ decreases due to the interaction between the different interface modes, before penetrating in the regions where the waves become propagative in vacuum and/or in LHM. One can also notice the existence of several branches of both TE and TM polarizations in the frequency range $\omega D/c \sim 4$ to 4.2 which are essentially slab modes of the LHM layers, because they fall in the regions where the modes are propagating in LHM but evanescent in vacuum. Similarly, the narrow bands that become asymptotic to the light line of vacuum when $k_{\parallel}D$ increases are essentially slab modes of the vacuum layers. Finally, one can recognize around $\omega D/c \simeq 4.5$ [see Fig. 8(b)] the existence of an omnidirectional band gap for TE polarization of the electromagnetic field. These general trends parallel those mentioned in the previous discussions. It is also interesting to mention that an omnidirectional band gap occurs in the TM band structure around $\omega D/c \simeq 7$ [see Fig. 8(a)]; however, in this frequency range only the dielectric permittivity ε_2 is negative while the magnetic permittivity μ_2 is positive.

IV. SUMMARY AND CONCLUSIONS

In this paper we have presented a detailed study of the photonic band structure of one-dimensional superlattices composed of alternate layers of right-handed and left-handed materials. The different possible behaviors have been illustrated by varying the physical parameters and the volume fraction of LHM materials. In particular, the formation of the bands below or between the light lines of the constituting materials can be understood on the basis of the localized interface modes at a LHM-RHM boundary and the confined modes of a LHM (RHM) layer sandwiched between two semi-infinite RHM (LHM). While the RHM-LHM layer can, in principle, support both TE and TM interface modes, only one of these modes can exist at most. Thus, in the superlat-tice band structure, there can be at most one band originating from the localized interface mode. Between the light lines of the constituting materials, there are also narrow bands originating from the confined modes of a layer, their number increasing with the volume fraction of the corresponding material in the superlattice. Among other peculiar behaviors associated with the presence of the LHM with fixed parameters ε_2 and μ_2, one can notice the behavior of the band structure in the vicinity of $\omega=0$ and, in particular, the existence of a band that lies below the light lines of the constituting materials and can reach a vanishing frequency at nonvanishing values of the wave vector $k_{\parallel}$. Also, the dispersion curves ω versus k_z, calculated for a given value of $k_{\parallel}$, do not behave always monotonically as in usual superlattices, but may describe only a limited range of the Brillouin zone and display a zigzag behavior. For specific values of the parameters, such bands may become even very narrow and appear as a discrete mode ω at $k_z=0$ or π/D. This happens, in particular, at $k_{\parallel} \cong 0$ when the average index of refraction in the superlattice is equal to zero, but such a behavior is not limited only to the case $\langle n \rangle = 0$.

Finally, a new phenomenon associated with the presence of the LHM is the possibility of an absolute band gap, of either TE or TM polarization, when the material parameters are chosen appropriately. This enables us to propose an application of our structure for realizing an omnidirectional optical mirror that prevents propagation of optical waves of TE or TM polarization for a given frequency range. Combination in tandem of two such multilayers can yield an omnidirectional reflector of light for both polarizations.

[1] J. B. Pendry, in *Photonic Crystals and Light Localization in the 21st Century*, edited by C. M. Soukoulis, Vol. 563 of NATO Science, Series C (Kluwer, Dordrecht 2002), p. 329; D. R. Smith, W. J. Padilla, D. C. Vier, R. Shelby, S. C. Nemat-Nasser, N. Kroll, and S. Schultz, *ibid.*, p. 351.

[2] V. G. Veselago, Sov. Phys. Usp. **10**, 509 (1968).

[3] R. A. Shelby, D. R. Smith, and S. Schultz, Science **292**, 77 (2001); R. A. Shelby, D. R. Smith, S. C. Nemat-Nasser, and S. Schultz, Appl. Phys. Lett. **78**, 489 (2001).

[4] R. Marqués, J. Martel, F. Mesa, and F. Medina, Phys. Rev. Lett. **89**, 183901 (2002); P. Gay-Balmaz and O. J. F. Martin, J. Appl. Phys. **92**, 2929 (2002).

[5] J. B. Pendry, A. J. Holden, D. J. Robbins, and W. J. Steweat, IEEE Trans. Microwave Theory Tech. **47**, 2075 (2000); J. M.

Pitarke, F. J. Garcia-Vidal, and J. B. Pendry, Phys. Rev. B **57**, 15 261 (1998).

[6] S. Foteinopoulou, E. N. Economou, and C. M. Soukoulis, Phys. Rev. Lett. **90**, 107402 (2003).

[7] A. A. Houck, J. B. Brock, and I. L. Chuang, Phys. Rev. Lett. **90**, 137401 (2003).

[8] C. G. Parazzoli, R. B. Greegor, K. Li, B. E. C. Koltenbah, and M. Tanielian, Phys. Rev. Lett. **90**, 107401 (2003).

[9] R. W. Ziolkowski and E. Heyman, Phys. Rev. E **64**, 056625 (2001).

[10] D. R. Smith, D. Schurig, and J. B. Pendry, Appl. Phys. Lett. **81**, 2713 (2002).

[11] J. B. Pendry, Phys. Rev. Lett. **85**, 3966 (2000).

[12] M. W. Feise, P. J. Bevelacqua, and J. B. Schneider, Phys. Rev.

B **66**, 035113 (2002).

[13] N. Fang and X. Zhang, Appl. Phys. Lett. **82**, 161 (2003).

[14] Z. M. Zhang and C. J. Fu, Appl. Phys. Lett. **80**, 1097 (2002).

[15] S. Enoch, G. Tayeb, P. Sabouroux, N. Guérin, and P. Vincent, Phys. Rev. Lett. **89**, 213902 (2002).

[16] I. S. Nefedov and S. A. Tretyakov, Phys. Rev. E **66**, 036611 (2002).

[17] J. Li, L. Zhou, C. T. Chan, and P. Sheng, Phys. Rev. Lett. **90**, 083901 (2003).

[18] L. Wu, S. He, and L. Shen, Phys. Rev. B **67**, 235103 (2003).

[19] J. N. Fink, S. Winn, S. Fan, C. Chen, J. Michel, J. D. Joannopoulos, and E. L. Thomas, Science **282**, 1679 (1998).

[20] J. P. Dowling, Science **282**, 1841 (1998).

[21] D. N. Chigrin, A. V. Lavrinenko, D. A. Yarotsky, and S. V. Gaponenko, Appl. Phys. A: Mater. Sci. Process. **68**, 25 (1999).

[22] D. Bria, B. Djafari-Rouhani, E. H. El Boudouti, A. Mir, A. Akjouj, and A. Nougaoui, J. Appl. Phys. **91**, 2569 (2002), and references therein.

[23] D. Bria, B. Djafari-Rouhani, A. Bousfia, E. H. El Boudouti, and A. Nougaoui, Europhys. Lett. **55**, 841 (2001); D. Bria and B. Djafari-Rouhani, Phys. Rev. E **66**, 056609 (2002).

[24] R. Ruppin, Phys. Lett. A **227**, 61 (2000).

[25] R. Ruppin, J. Phys.: Condens. Matter **13**, 1811 (2001).

[26] M. L. Bah, A. Akjouj, and L. Dobrzynski, Surf. Sci. Rep. **16**, 95 (1992).